A Collapsed Intermediate with Nonnative Packing of Hydrophobic Residues in the Folding of TEM-1 β-Lactamase[†]

Marc Vanhove,*[,‡,§] Annabelle Lejeune,[‡] Gilliane Guillaume,[‡] Richard Virden,[||] Roger H. Pain,[⊥] Franz X. Schmid,[#] and Jean-Marie Frère[‡]

Laboratoire d'Enzymologie and Centre d'Ingénierie des Protéines, Institut de Chimie B6, Université de Liège, Sart-Tilman, B-4000 Liège, Belgium, Department of Biochemistry and Genetics, University of Newcastle upon Tyne, NE2 4HH, United Kingdom, Department of Biochemistry and Molecular Biology, Jožef Stefan Institute, SLO-1111 Ljubljana, Slovenia, and Laboratorium für Biochemie, Universität Bayreuth, D-8580 Bayreuth, Germany

Received August 28, 1997; Revised Manuscript Received December 8, 1997

ABSTRACT: The kinetics of refolding of TEM-1 β-lactamase from solution in guanidine hydrochloride have been investigated on the manual and stopped-flow mixing time scales. The kinetics of change of far-UV circular dichroism and of intrinsic and ANS fluorescence have been compared with changes in the quenching of fluorescence by acrylamide as a probe of the accessibility of solvent to tryptophan. The binding of ANS points to hydrophobic collapse in the very early stages of folding which take place in the burst phase. This is accompanied by regain of 60−65% of native ellipticity, indicating formation of a significant proportion of secondary structure. Also in the burst phase, the tryptophan residues, which are largely exposed to solvent in the native protein, become less accessible to acrylamide, and the intrinsic fluorescence increases markedly. An early intermediate is thus formed in which tryptophan is more buried than in the native protein. Further intermediates are formed over the next 20 s. Quenching by acrylamide increases during this period, as the transient nonnative state is disrupted and the tryptophan residue(s) become(s) reexposed to solvent. The two slowest phases are determined by the isomerization of incorrect prolyl isomers, but double jump tryptophan fluorescence and acrylamide quenching experiments show little, if any, effect of proline isomerization on the earlier phases. Hydrophobic collapse thus occurs to a folding intermediate in which there is a nonnative element of structure which has to rearrange in the later steps of folding, resulting in a nonhierarchical folding pathway. The C-terminal W290 is suggested as being involved in the nonnative intermediate. β-Lactamase provides further evidence for the occurrence of nonnative intermediates in protein folding.

In recent years, our knowledge of the mechanisms by which a polypeptide chain folds into its native conformation in vitro has progressed significantly. This is due mainly to the development of complementary fast-reaction techniques which can monitor structural changes taking place along the folding pathway (*1*−*3*). Although some proteins such as the chymotrypsin inhibitor CI2 (*4*, *5*), ubiquitin (*6*), the acyl-coenzyme A binding protein (*7*), and the cold-shock protein from *Bacillus subtilis* CspB (*8*) can fold rapidly and in a highly cooperative manner, the folding of many proteins involves detectable intermediates and even multiple pathways (*9*−*12*). The formation of stable hydrogen-bonded structures has been studied by quenched-flow hydrogen exchange monitored by NMR (*1*, *13*−*14*), the populations of species present during folding have been deduced by electrospray ionization mass spectrometry (*15*), and spectroscopic probes linked with fast-mixing technology have led to characterization of rapid conformational changes (*3*, *16*−*20*). A number of distinct kinetic phases are commonly observed in such studies, including hydrophobic collapse and the rapid formation of large proportions of nativelike secondary structure within stopped-flow dead-times, prior to the slower development of stabilizing interactions leading to the formation of the native state (*2*).

The common observation of a "burst" phase in the formation of secondary structure, together with the submicrosecond time range for the helix−coil transition (*21*, *22*), is consistent with a framework model in which the polypeptide chain undergoes local folding to nativelike secondary structures which direct subsequent folding through diffusion/collision processes (*23*−*25*). In an alternative model, the association of nonpolar side chains induces a hydrophobic collapse of the polypeptide to a compact species in which secondary structure is more readily formed (*26*, *27*). This model is supported by several recent reports of

[†] This work was supported by the Belgian Government in the frame of the Pôle d'Attraction Interuniversitaire (PAI no.19) and Actions Concertées 89−94/130 and #93-98/170, and by the Fonds de la Recherche Scientifique Medicale (Contract 3.4537.88). M.V. was the recipient of an EMBO short-term fellowship during his stay at the University of Bayreuth.

* To whom correspondence should be addressed.

[‡] Université de Liège.

[§] Present address: Department of Tumor Cell Biology, St. Jude Children's Research Hospital, 332 N. Lauderdale, Memphis, TN 38105. Telephone: 901-495-2446. Fax: 901-495-2381. E-mail: marc.vanhove@stjude.org.

[||] University of Newcastle upon Tyne.

[⊥] Jožef Stefan Institute.

[#] Universität Bayreuth.

S0006-2960(97)02143-0 CCC: $15.00
Published on Web 01/27/1998

FIGURE 1: Stereo α-carbon trace of TEM-1 β-lactamase showing the positions of the four tryptophan residues (*45*, *46*). The distance between Cζ3 Trp229 and Cϵ3 Trp290 is 0.378 nm.

residual structure in the 434 repressor (*28*), the α-subunit of tryptophan synthase (*29*), and staphylococcal β-lactamase (*30*) in high concentrations of denaturant, which suggests that the association of nonpolar side chains may be an important early event in folding. The development of nonpolar surfaces, as evidenced by the binding of the hydrophobic fluorescent probe ANS[1] (*17*, *31*), is consistent with early formation of the hydrophobic core of the protein. The fact that both occur within the dead-time of existing equipment makes it currently impossible to determine whether hydrophobic collapse precedes the formation of secondary structure or *vice versa*, although the development of ultra-rapid mixing, photoinitiated reactions, and temperature-jump-induced refolding may provide a means of resolving this question (*32*).

In either model, it is possible to envisage a pathway involving intermediates with structures and interactions not found in the native state. Transient, nonnative α-helical structure was indeed found early in the folding of β-lactoglobulin (*33*), and a nonnative intermediate involving tryptophan residues reported for lysozyme (*10*, *20*, *34*) has since been further characterized (*35*). It is important to ask whether, as suggested (*35*), this is a more general phenomenon.

TEM-1 β-lactamase is a well-characterized enzyme of molecular mass 28 907 Da whose structure is shown in Figure 1. In this further study of its folding kinetics, we present evidence for the early hydrophobic collapse to a folding intermediate which contains nonnative structure involving tryptophan.

MATERIALS AND METHODS

Enzyme and Reagents. TEM-1 β-lactamase was produced by *Escherichia coli* strain RB 791 (*36*) and purified as described by Dubus et al. (*37*). Ultrapure guanidinium chloride (GdmCl) was from Schwarz/Mann (Orangeburg, NJ). GdmCl concentrations were determined by refractive index measurement (*38*). Acrylamide was from Serva (Heidelberg, Germany), and 1-anilino-8-naphthalenesulfonic acid (ANS) was from Sigma. Other chemicals were of reagent grade. Unless otherwise stated, experiments were performed at 25 °C using 50 mM sodium phosphate, 50 mM NaCl, pH 7, as refolding buffer. GdmCl solutions were prepared in the same buffer, the pH being adjusted as necessary.

[1] Abbreviations: GdmCl, guanidinium chloride; ANS, 1-anilino-8-naphthalenesulfonic acid; CD, circular dichroism.

Fluorescence Measurements. Intrinsic tryptophan fluorescence was monitored using a Perkin-Elmer LS50 spectrofluorometer, with excitation and emission wavelengths of 280 and 340 nm, respectively. Bandwidths were 4 nm for both excitation and emission. Protein concentration was 3 μM. ANS fluorescence was similarly monitored at 480 nm with excitation at 380 nm. Bandwidths were 4 nm for excitation and 10 or 20 nm for emission. Protein and ANS concentrations in the cuvette were 3.3 μM and 60 μM, respectively. For refolding experiments, the enzyme was unfolded for at least 1 h in 3 M GdmCl and diluted 11-fold with the refolding buffer. Acrylamide (final concentration, 0.182 M) or ANS was added in the refolding buffer as required. In the former case, parallel folding runs in the absence of acrylamide allowed F_0/F, the ratio of fluorescence in the absence and presence of quencher, to be calculated as a function of time. The manual mixing dead-time was approximately 15 s. The fluorescence intensity of the fully unfolded enzyme under refolding conditions (0.273 M GdmCl) was estimated by extrapolation of the fluorescence of the protein measured at various GdmCl concentrations between 3 and 6 M. For acrylamide quenching experiments, F_0/F for the fully unfolded protein was deduced from the fluorescence intensity of the protein in 3.0 M GdmCl, measured either in the presence or in the absence of acrylamide. These controls were done independently for manual and stopped-flow conditions.

Fluorescence Stopped-Flow Kinetics. Unless otherwise stated, a DX 17MV sequential mixing stopped-flow spectrometer from Applied Photophysics (Leatherhead, U.K.) was used. The path length of the observation cuvette was 2 mm. Refolding reactions were initiated by an 11-fold dilution of the protein, previously denatured in 3 M GdmCl, with refolding buffer. Changes of the intrinsic tryptophan fluorescence were followed by monitoring the total fluorescence above 300 nm, with excitation at 280 nm (4.65 nm bandwidth). Scattered light from the excitation beam was absorbed by an aqueous solution of cytidine 2′-phosphate in a 0.2 cm cell inserted between the observation chamber and the emission photomultiplier. Protein concentration was 3 μM. Acrylamide quenching as a function of time was analyzed as described above.

Total ANS fluorescence was measured above 400 nm (with excitation at 380 nm, 4.65 nm bandwidth), using an aqueous solution of ANS to absorb scattered light. ANS was included in the refolding buffer, and the final protein and ANS concentrations were 3.3 μM and 60 μM, respec-

Table 1: Kinetic Parameters for the Refolding of TEM-1 β-Lactamase in 0.273 M GdmCl[i]

probe	burst phase	phase 1	phase 2	phase 3	phase 4	phase 5
Trp fl[a]						
k (s^{-1})	>1000	6.2 ± 0.4	1.6 ± 0.1	0.18 ± 0.002	0.031 ± 0.003	0.0036 ± 0.0001
amplitude	0.20 ± 0.01	−0.073 ± 0.003	−0.098 ± 0.003	0.19 ± 0.001	0.31 ± 0.02[g]	0.47 ± 0.05[g]
Trp fl-DJ 10 min[b]						
k (s^{-1})	>1000	6.9 ± 0.6	1.5 ± 0.1	0.15 ± 0.006	0.03[h]	nd[j]
amplitude	0.29 ± 0.02	−0.15 ± 0.01	−0.17 ± 0.01	0.22 ± 0.003	0.35 ± 0.006	
Trp fl-DJ 5 min[b]						
k (s^{-1})	>1000	7.9 ± 0.4	1.5 ± 0.1	0.15 ± 0.004	0.03[h]	nd
amplitude	0.28 ± 0.02	−0.15 ± 0.005	−0.17 ± 0.01	0.21 ± 0.002	0.33 ± 0.004	
Trp fl-DJ 5 s[b]						
k (s^{-1})	>1000	10.3 ± 1.0	2.2 ± 0.1	0.20 ± 0.002	0.03[h]	nd
amplitude	0.29 ± 0.02	−0.20 ± 0.01	−0.24 ± 0.01	1.00 ± 0.003	0.11 ± 0.005	
acryl[c]						
k (s^{-1})	>1000	4.8 ± 1.8	1.2 ± 0.2	0.19 ± 0.01	0.032 ± 0.006	0.0034 ± 0.0006
amplitude	−0.96 ± 0.04	0.05 ± 0.02	0.10 ± 0.02	0.19 ± 0.006	0.8 ± 0.2	−0.11 ± 0.05
acryl DJ 10 min[d]						
k (s^{-1})	>1000	5.3 ± 2.6	1.1 ± 0.4	0.14 ± 0.03	0.03[h]	nd
amplitude	−1.1 ± 0.04	0.06 ± 0.02	0.10 ± 0.02	0.16 ± 0.01	0.24 ± 0.02	
acryl DJ 5 min[d]						
k (s^{-1})	>1000	6.0 ± 3.4	0.9 ± 0.2	0.11 ± 0.03	0.03[h]	nd
amplitude	−1.1 ± 0.04	0.03 ± 0.01	0.09 ± 0.01	0.14 ± 0.02	0.20 ± 0.03	
acry DJ 5 s[d]						
k (s^{-1})	>1000	2.1 ± 0.6	0.7 ± 0.1	0.07 ± 0.02	0.03[h]	nd
amplitude	−1.1 ± 0.03	0.11 ± 0.05	0.25 ± 0.05	0.15 ± 0.03	−0.01 ± 0.004	
ANS fl[e]						
k (s^{-1})	>1000	6.6 ± 0.2	1.4 ± 0.03	0.18 ± 0.003	0.033 ± 0.001	0.0034 ± 0.0001
amplitude	9.9 ± 0.06	−1.5 ± 0.02	−1.9 ± 0.02	−1.4 ± 0.01	−4.9 ± 0.3	−3.0 ± 0.3
Far-UV CD[f]						
k (s^{-1})	>300	15 ± 2	0.9 ± 0.2	0.057 ± 0.003	−	−
amplitude	0.62 ± 0.03	0.14 ± 0.02	0.10 ± 0.01	0.14 ± 0.003		

[a] Intrinsic tryptophan fluorescence. [b] Intrinsic fluorescence followed after unfolding for the time stated. [c] Quenching of fluorescence by acrylamide. [d] Quenching of fluorescence by acrylamide followed after unfolding for the time stated. [e] ANS fluorescence. [f] Circular dichroism at 225 nm. [g] Corrected so that the total amplitude change is equal to unity. [h] The value of 0.03 s^{-1} is the average value for phase 4 measured in single jump manual mixing kinetics; corresponding amplitudes are from stopped-flow data. [i] Data for the burst phase and phases 1, 2, and 3 are from stopped-flow experiments; standard errors (95% confidence limit) are from nonlinear least-squares analysis. Data for phases 4 and 5 are from manual mixing experiments (see text); errors are standard deviations from the average of three runs. Experiments were performed at 25 °C (21 °C for the CD experiments). The signs of the amplitudes derived from eqs 1, 2, and 3 have been reversed so that an increase of the measured parameter is denoted by a positive amplitude. [j] nd, not determined.

tively. The photomultiplier voltage was set to 750 V in all experiments.

Usually, 13−14 traces were averaged. Good resolution of the initial stages of the kinetics was achieved by "splitting" the time base, i.e., by accumulating more data points during the early times of the reaction.

The mixing dead-time of the stopped-flow instrument was measured using the reaction between 2,6-dichlorophenolindophenol and L-ascorbic acid (*39*), and was in the 3−4 ms range. To test the absence of mixing artifacts, the enzyme was replaced by a 12 μM tryptophan solution, and experiments were performed as described above.

Far-UV CD-Detected Stopped-Flow Refolding Kinetics. A stopped-flow spectrophotometer with a dual monochromator (bandwidth 2.3 nm) was fitted with a calcite modulator accessory (Applied Photophysics Model SX-17MV) and a 150 W mercury−xenon lamp (Hamamatsu Photonics Model L2482). Ellipticity was followed at 225 nm using a 2 mm light path sample-cell. The dead-time calculated from the measured flow rate was 12−13 ms. A solution (1 mg/mL) of (1*S*)-(+)-10-camphorsulfonic acid was used to calibrate the CD signal. Refolding was initiated in a 200 μL sample by an 11-fold dilution into the refolding buffer of the protein, previously unfolded for at least 1 h in 3 M GdmCl. Final β-lactamase concentration was 8.5 μM. Experiments were performed at 20.5−21 °C. The ellipticity of the unfolded protein was measured at 3 M GdmCl.

Stopped-Flow Double-Mixing Experiments. The protein (160 μM) was first unfolded by a 1:5 mixing with 3.6 M GdmCl, and then refolded, after the desired delay time, by a second, 1:5 mixing with the refolding buffer containing 0.24 M ammonium sulfate and, where required, 0.22 M acrylamide. Final protein, GdmCl, ammonium sulfate, and acrylamide concentrations were thus 3 μM and 0.5, 0.2, and 0.183 M, respectively. Refolding was followed by monitoring changes in the integrated tryptophan fluorescence above 300 nm, with excitation at 280 nm (4.65 nm bandwidth). The photomultiplier voltage was set at 750 V.

Control experiments of 1:5 mixing of the protein with 3.6 M GdmCl and monitoring unfolding by fluorescence and by ellipticity at 225 nm showed that 5 s incubation in 3 M GdmCl was sufficient to completely unfold the protein.

The fluorescence of the fully unfolded protein under refolding conditions (0.5 M GdmCl and 0.2 M ammonium sulfate) was estimated by extrapolation of the protein fluorescence measured at GdmCl concentrations between 3 and 6 M. F_0/F for the unfolded protein is the ratio of the fluorescence signals in the absence and presence of acrylamide as measured in 3 M GdmCl.

Data Analysis. GraFit (Erithacus Software) was used for nonlinear least-squares analyses. The refolding kinetics reported in Table 1 as being composed of a burst phase and five measurable phases were obtained from stopped-flow (k_1-k_4) and manual mixing (k'_4, k'_5) experiments and were

analyzed by eqs 1 and 2, respectively. k'_4 corresponds to the faster phase observed by manual mixing, and k_4 was fixed to this value. The slowest phase observed by manual mixing was at least 50 times slower than the slowest events recorded by stopped-flow, and was therefore ignored when analyzing stopped-flow refolding data.

Refolding kinetics obtained by monitoring the ellipticity at 225 nm were analyzed according to a sum of three exponentials (eq 3).

$$F_{obs} = A_1 \exp(-k_1 t) + A_2 \exp(-k_2 t) + A_3 \exp(-k_3 t) + A_4 \exp(-k_4 t) + F_\infty \quad (1)$$

$$F_{obs} = A'_4 \exp(-k'_4 t) + A'_5 \exp(-k'_5 t) + F_\infty \quad (2)$$

$$CD_{obs} = A_1 \exp(-k_1 t) + A_2 \exp(-k_2 t) + A_3 \exp(-k_3 t) + CD_\infty \quad (3)$$

RESULTS

The structures of transient intermediates were probed using a combination of spectroscopic techniques including intrinsic fluorescence, fluorescence quenching by acrylamide, fluorescence-detected binding of ANS, and far-UV circular dichroism. The refolding conditions were 0.273 M GdmCl, 50 mM sodium phosphate, 50 mM NaCl, pH 7.0 at 25 °C (20.5−21 °C for the CD experiments).

Intrinsic Fluorescence. The intrinsic fluorescence of TEM-1 enzyme is dominated by the four tryptophan residues, and changes in fluorescence intensity occurring during folding can be readily monitored (*40*). In these experiments, tyrosines, of which there are four, are also excited, but the emission spectrum (*40*) indicates that most or all of the energy absorbed by these residues is quenched in the native state. This has little effect on the tryptophan fluorescence of most folded proteins (ref *41*, pp 347−350). The potentially larger contribution from tyrosine fluorescence in partially folded or unfolded states does not complicate the kinetics in this case, as shown by the agreement between the values of stopped-flow rate constants monitored by intrinsic and ANS fluorescence (Table 1). The relative amplitudes could, however, involve small contributions from tyrosine.

The first 50 s of the refolding reaction monitored by stopped-flow mixing and the total refolding time monitored by manual mixing, each normalized relative to the unfolded state under refolding conditions, are shown in Figure 2A and Figure 2B, respectively. Overall, the refolding of TEM-1 enzyme monitored by the intrinsic fluorescence exhibits six distinct phases including the burst phase which takes place within the dead-time of mixing. The first four measurable phases (k_1−k_4) are observed in the stopped-flow experiments and the fourth and fifth (k_4 and k_5) in the manual mixing experiments. The fourth phase is common to both, and the stopped-flow data are fitted using the value of k'_4 obtained from the manual data. The accuracy of the fits (see Materials and Methods) is demonstrated by the random distribution of residuals as shown in Figure 2. When data from stopped-flow experiments were analyzed with only three exponentials, the accuracy of the fit was significantly poorer, as seen from the distribution of residuals in Figure 2A (ii).

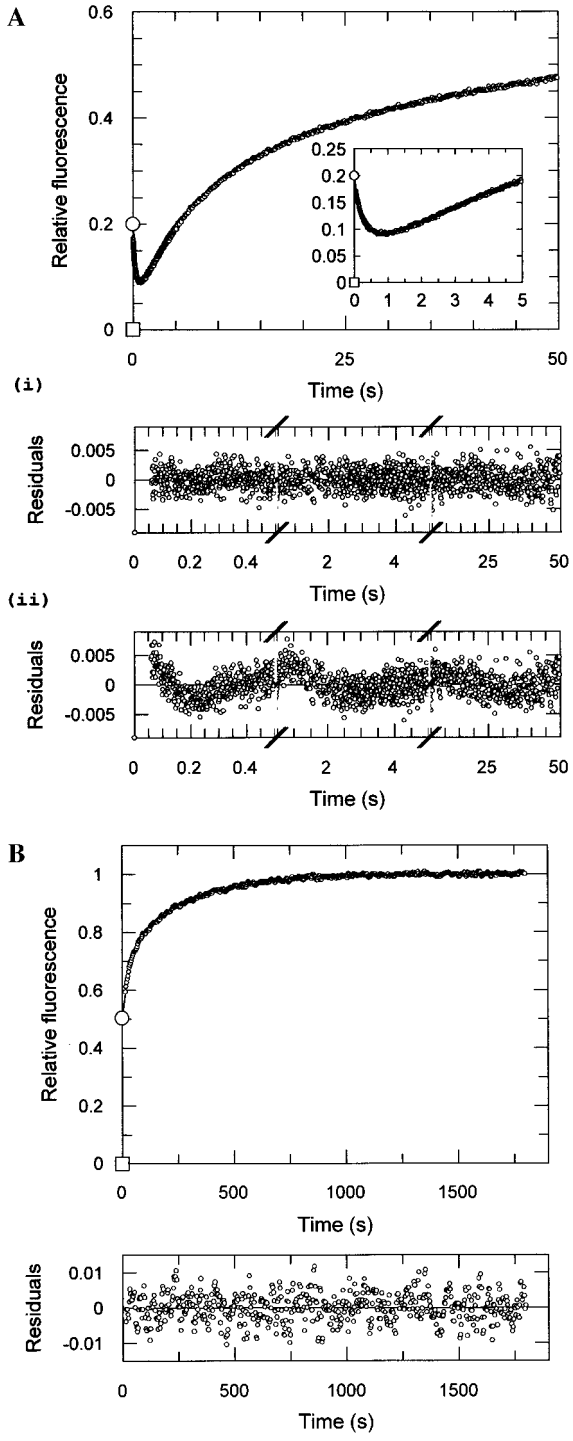

FIGURE 2: Refolding kinetics of TEM-1 β-lactamase monitored by intrinsic tryptophan fluorescence. Refolding was carried out in 0.273 M GdmCl, 50 mM sodium phosphate, 50 mM NaCl, pH 7.0 at 25 °C, by an 11-fold dilution of the protein previously unfolded in 3 M GdmCl. The fluorescence emission was normalized relative to that of the unfolded protein under the same conditions, so that the value of the denatured state (see Materials and Methods) is 0 (represented by □) and that of the native state is 1. (A) Stopped-flow mixing: the total fluorescence above 300 nm was measured. The inset shows the first 5 s of the reaction. (B) Manual mixing: fluorescence was recorded at 340 nm. Excitation was at 280 nm in both cases. The solid lines represent the fit of the data (A) to a sum of four exponentials and (B) to a sum of two exponentials (see Materials and Methods and Table 1). Panels A(i) and A(ii) show residuals from the fit of the experimental data to four- and three-exponential equations, respectively. (○) Intrinsic fluorescence extrapolated to zero time from the kinetic data.

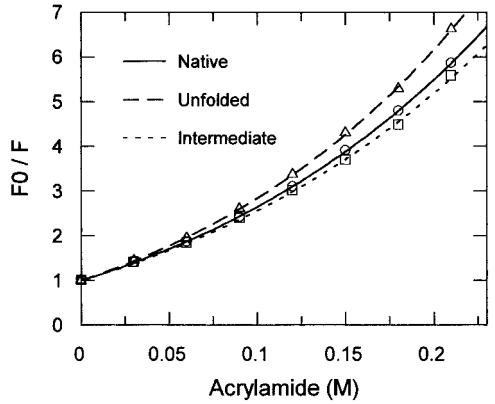

FIGURE 3: Stern−Volmer plots of F_0/F vs quencher concentration for the native state of TEM-1 β-lactamase in 0.273 M GdmCl (○), the thermodynamically stable intermediate in 1.4 M GdmCl (□), and the unfolded state in 3 M GdmCl (△). F and F_0 are the fluorescence intensities in the presence and absence, respectively, of acrylamide.

The refolding rate constants and amplitudes are summarized in Table 1. First, during the dead-time of the experiment, the fluorescence rapidly increases in an initial "burst" phase whose amplitude accounts for 20% of the net increase in fluorescence. A subsequent decrease in fluorescence occurs in two phases to reach a minimum in 800 ms, indicating the accumulation of intermediates with lower fluorescence quantum yields. This is followed by a final increase in three phases to the fluorescence intensity of the native state.

Quenching of Fluorescence by Acrylamide. The above results show that significant changes in environment of at least some of the four tryptophan residues occur during folding. The different conformational changes involved cannot, however, be differentiated, because the total fluorescence intensity above 300 nm depends on a variety of factors (*42*). To focus on the rate at which tryptophan residues become sequestered from solvent, and thus act as probes of hydrophobic collapse, refolding of the protein can be followed in the presence of a fluorescence quenching agent (*20, 43, 44*). Acrylamide was used, rather than iodide, to avoid the possible effects of ionic strength on the folding process (*20*). Refolding kinetics followed by recovery of enzyme activity were independent of the presence of 0.2 M acrylamide, showing that at least the late steps of the folding reaction were unaffected by the quenching agent. Although acrylamide might be expected to affect the stability of folding intermediates, closely similar rate constants for all phases were obtained when either 0.3 M potassium iodide as quencher or 0.3 M KCl as control was used (results not shown).

The tryptophan residues in TEM-1 β-lactamase are located on the surface of the protein, three out of four being highly solvent-accessible (*45, 46*), in keeping with the small red-shift as the protein unfolds [λ_{max} = 347, 352, and 356 nm for N, H, and U respectively (*40*)]. The solvent accessibility is established by the Stern−Volmer plots presented in Figure 3. The plots for the native enzyme, the fully unfolded protein, and the thermodynamically stable intermediate state H (*40*) display upward curvature (Figure 3), indicating significant contributions from both dynamic and static quenching (*47*). This is taken into account by the modified Stern−Volmer equation (*47, 48*)

$$F_0/F = (1 + K_{SV}[Q])e^{V[Q]} \quad (4)$$

where K_{SV} is the Stern−Volmer constant for the dynamic quenching process and V is the static quenching constant. The values of K_{SV} and V obtained by nonlinear regression of the data in Figure 3 are listed in Table 2. The K_{SV} values for the native enzyme and the stable intermediate are identical within experimental error and very close to that of the unfolded protein, showing that the tryptophan residues in the two former species are almost completely solvent-exposed. Furthermore, the nonzero V values for each species suggest that acrylamide binds in the vicinity of the tryptophan residues and induces static quenching.

Table 2: Stern−Volmer (K_{SV}) and Static Quenching (V) Constants for the Fluorescence Quenching of TEM-1 β-Lactamase by Acrylamide[a]

state	K_{SV} (M^{-1})	V (M^{-1})
native (in 0.273 M GdmCl)	8.7 ± 0.2	3.5 ± 0.1
stable intermediate H (in 1.4 M GdmCl)	8.4 ± 0.6	3.3 ± 0.3
unfolded (in 3 M GdmCl)	9.4 ± 0.4	3.8 ± 0.2

[a] Values are calculated from the data in Figure 3. Errors are standard deviations (95% confidence limit) from the nonlinear least-squares analyses.

The change of solvent accessibility of tryptophan residues during folding was followed by monitoring fluorescence in the presence of 0.182 M acrylamide. The ratio of the fluorescence intensity in the absence of acrylamide to that in its presence (F_0/F) is plotted as a function of time in Figure 4. A decrease in F_0/F reflects sequestering of tryptophan residues from solvent. The differences in the F_0/F values in Figure 4A (stopped-flow mixing) and Figure 4B (manual mixing) arise from the different emission bandwidths but do not affect the analysis of the kinetics.

The data in Figure 4A,B were analyzed according to sums of four and two exponentials, respectively (eqs 1 and 2), and the results are listed in Table 1. Due to a lower signal-to-noise ratio, data from Figure 4A could also be satisfactorily fitted to the sum of three exponentials, but the present interpretation was preferred on the basis of the good agreement of the calculated rate constants with those obtained from Figure 2A. In the burst phase, a very large decrease in F_0/F is observed. F_0/F subsequently increases in four successive phases. The last phase has a small, negative amplitude, so that F_0/F exhibits a maximum at about 120 s. On average then, tryptophan residues are sequestered from solvent during the first 3−4 ms, then more slowly reexposed to solvent as the protein folds, finally undergoing a slight reduction in exposure as the protein packs to its native conformation.

The possibility that the decrease in F_0/F observed in the earliest stages of folding reflects transient intermolecular association with consequent burial of tryptophan was investigated by measuring the dependence of protein concentration on the refolding kinetics (Table 3). Data from Table 3 were obtained under different experimental conditions (see legend) and differ slightly from those in Table 1. However, these results show clearly that there is no effect of protein

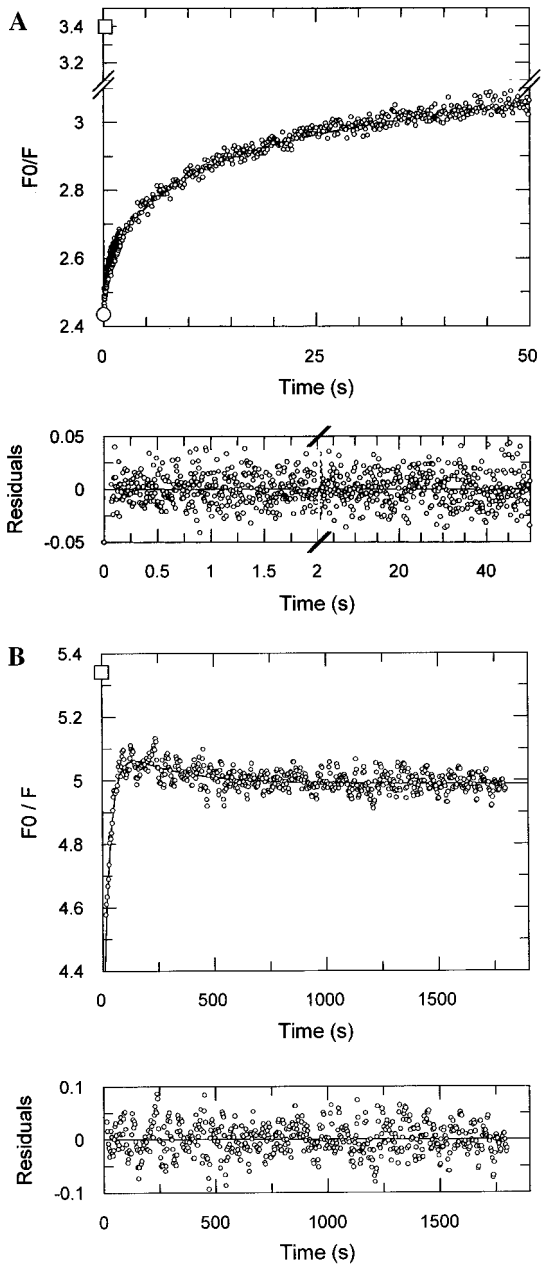

FIGURE 4: Quenching of intrinsic fluorescence by 0.182 M acrylamide during refolding of TEM-1 β-lactamase. Refolding was carried out in 0.273 M GdmCl, 50 mM sodium phosphate, 50 mM NaCl, pH 7.0 at 25 °C. The data are plotted as the ratio of the intrinsic fluorescence in the absence of acrylamide (F_0) to that in the presence of quencher (F). (A) Stopped-flow; (B) manual mixing. Experimental conditions were as described in the legend of Figure 2. The solid lines represent the fit of the experimental data (A) to a sum of four exponentials and (B) to a sum of two exponentials (see text and Table 1). Residuals are shown in the lower panels. (○) F_0/F extrapolated to zero time from the kinetic data; (□) F_0/F for the unfolded protein measured as the ratio of the fluorescence values at 3 M GdmCl, with and without acrylamide.

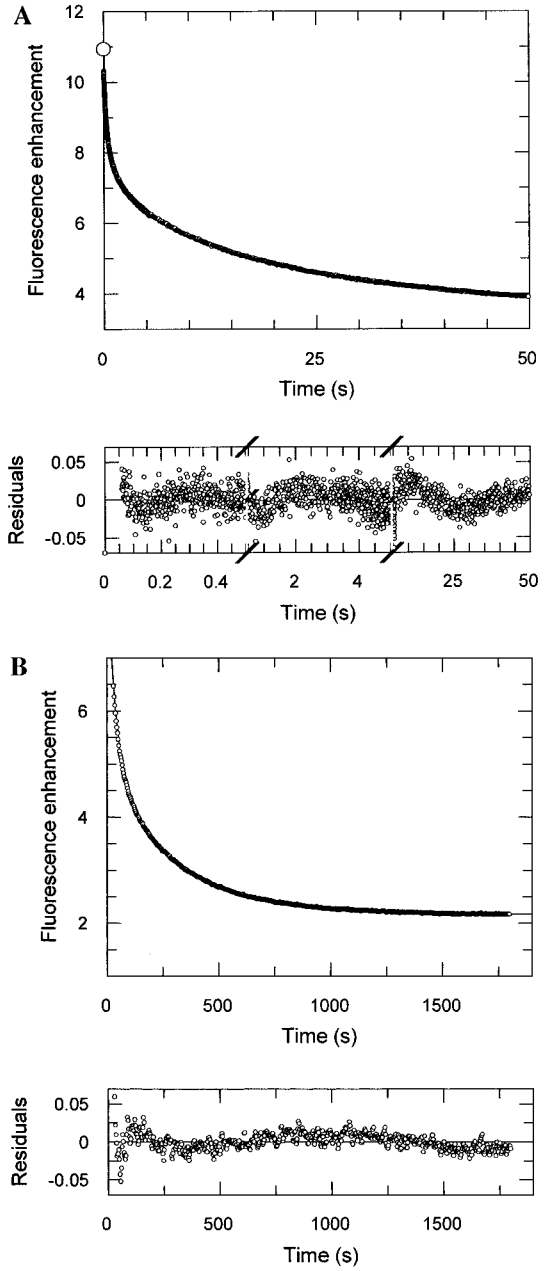

FIGURE 5: Refolding of TEM-1 β-lactamase (3.3 μM) monitored by the change in fluorescence intensity of ANS (60 μM) in 0.273 M GdmCl, 50 mM sodium phosphate, 50 mM NaCl, pH 7.0 at 25 °C. (A) Stopped-flow, total fluorescence above 400 nm; (○) signal extrapolated to zero time from the kinetic data. (B) manual mixing, fluorescence monitored at 480 nm. The excitation wavelength was 380 nm in each case. Fluorescence intensities are expressed relative to that of ANS in the absence of protein, measured under the relevant conditions. Folding conditions were as in the legend of Figure 2. The solid curves represent (A) the sum of four exponentials and (B) the sum of two exponentials (see Table 1). Residuals are given in the lower panels.

concentration on the rates or amplitudes of the different phases (including the burst phase). The early burial of tryptophans therefore takes place within a monomeric species.

ANS Binding. ANS binding provides a useful though empirical probe for following the condensation of nonpolar groups from the initial hydrophobic collapse to the tightly packed hydrophobic core characteristic of the native conformation. The increase in the intensity of ANS fluorescence observed during the folding of a number of proteins has been attributed to the formation of molten globule states, whose more mobile packing apparently favors the binding of the dye (*17, 31*).

The changes in the fluorescence intensity of ANS during the folding of TEM-1 β-lactamase were measured by including the dye in the refolding buffer. The unfolded protein in 3 M GdmCl causes no significant ANS fluores-

Table 3: Effect of Protein Concentration on the Refolding Kinetics of TEM-1 β-Lactamase Monitored by Acrylamide Quenching[a]

protein concn	burst phase	phase 1	phase 2	phase 3	phase 4	phase 5
1.2 μM						
k (s^{-1})	>500	13 ± 4	2.4 ± 0.3	0.18 ± 0.008	0.043 ± 0.006	0.0018 ± 0.0005
amplitude	-0.85 ± 0.03	0.04 ± 0.02	0.09 ± 0.01	0.10 ± 0.002	1.0 ± 0.1	-0.79 ± 0.15
7.5 μM						
k (s^{-1})	>500	13 ± 3	3.0 ± 0.3	0.25 ± 0.007	0.037 ± 0.005	0.0028 ± 0.0003
amplitude	-0.89 ± 0.02	0.04 ± 0.01	0.08 ± 0.01	0.09 ± 0.002	1.2 ± 0.06	-0.66 ± 0.06

[a] General conditions are those of Figure 4A,B except (1) that stopped-flow data were obtained on a Bio-Logic SFM-3 stopped-flow spectrometer [λ_{ex} = 280 nm (8 nm bandwidth); λ_{em} > 320 nm; path length of the observation cuvette = 1.5 mm; dead-time = 5.2 ms] and (2) that the bandwidth for fluorescence emission was 7 nm in the manual mixing experiments. Traces were analyzed as in Figure 4A,B. Data for the burst phase and phases 1, 2, and 3 are from stopped-flow experiments; standard errors (95% confidence limit) are from nonlinear least-squares analysis. Data for phases 4 and 5 are from manual mixing experiments; errors are standard deviations from the average of four runs. The signs of the amplitudes derived from eqs 1 and 2 have been reversed so that an increase of the measured parameter is denoted by a positive amplitude.

cence enhancement, and, assuming that this is also true in refolding buffer, the fluorescence of free ANS (value of unity) in Figure 5 is also that of the unfolded state. A dramatic increase in fluorescence intensity over that of free ANS is thus observed within the mixing dead-time of 3−4 ms. As in the case of intrinsic fluorescence, the burst phase reaction is followed by a five-exponential decrease to the values observed for the native enzyme, and the rate constants are listed in Table 1. It is possible that the binding of the probe to early intermediates could perturb the rate of their subsequent transformation into more nativelike species, and such an effect has been reported recently for lysozyme (*20*). Better fits—as judged by improved distribution of the residuals—may be obtained by analyzing data from Figure 5A,B with an additional exponential phase, and therefore the possibility that ANS slightly alters the folding kinetics cannot be ruled out unequivocally. However, the close similarity of the rate constants obtained from ANS binding to those obtained using the two other probes (Table 1) strongly suggests that, as for dihydrofolate reductase (*49*), the presence of ANS does not significantly affect the kinetics of folding.

Far-UV CD. The kinetics of formation of secondary structure were followed by stopped-flow circular dichroism in the far-UV, using the same folding conditions as for the other probes; 60−65% of the native ellipticity was generated within the mixing dead-time (Figure 6), indicating that a significant amount of secondary structure is formed within the burst phase. The kinetics for the subsequent folding are fitted by the sum of three exponentials with the rate constants given in Table 1. In contrast to fluorescence which detected additional slower phases, ellipticity reached its native value at the end of these three phases.

Double Jump Kinetics. The slow phases of folding for TEM-1 β-lactamase, which contains 12 proline residues, are the result of *cis*−*trans* isomerization of Xaa−Pro bonds (*40, 50*). To investigate the possible effect of proline isomerization on the kinetics of the early phases, folding from the unfolded chain containing the native isomers has been followed, using the double jump technique (*51, 52*) in which the protein is fully unfolded for a time much shorter than that required for proline isomerization and then immediately refolded. The β-lactamase was unfolded for times ranging from 5 s to 10 min in 3 M GdmCl at 25 °C (k_{unf} = 1.39 ± 0.05 s^{-1} from stopped-flow CD and intrinsic fluorescence kinetics) and refolding then initiated by a 1:5 dilution into refolding buffer containing 0.24 M ammonium sulfate, as

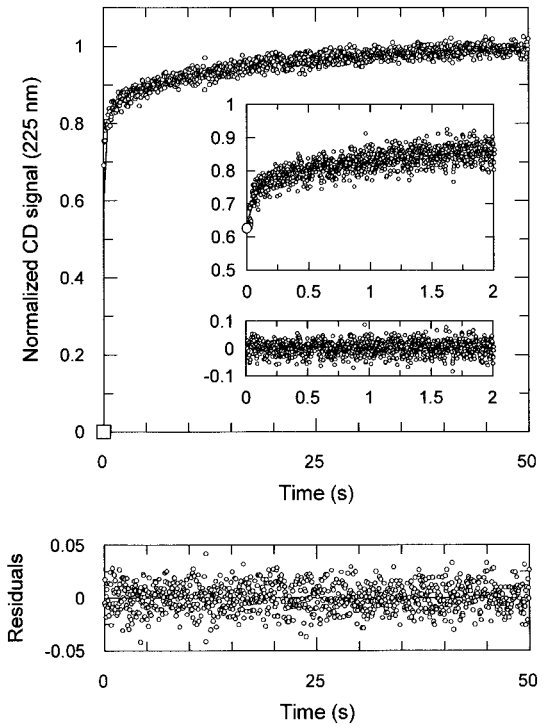

FIGURE 6: Refolding kinetics of TEM-1 β-lactamase monitored by stopped-flow CD at 225 nm in 0.273 M GdmCl, 50 mM sodium phosphate, 50 mM NaCl, pH 7.0 at 21 °C. The data, the average of 6 shots (0−50 s trace) and 21 shots (0−2 s trace, inset), were normalized to give the fractional values of native ellipticity. The signal for the fully unfolded protein is represented by □; see Materials and Methods. The curves are fits to the sum of three exponentials (see Table 1). Residuals are shown in the lower panels. (○) The signal extrapolated to zero time from the kinetic data. Refolding was initiated by 11-fold dilution of the protein (93.5 μM) unfolded in 3 M GdmCl.

described under Materials and Methods. This approach was necessary because the configuration of the stopped-flow mixing system precluded the use of the 1:10 dilution for the double jump routine. It has been well established for β-lactamase that sulfate will thermodynamically reverse the unfolding by denaturant (*53*). The concentration of sulfate was chosen to give the same refolding kinetics in a refolding solution containing 0.5 M GdmCl as in the 0.273 M GdmCl buffer used for the single jump experiments. This approach is justified by comparison of the kinetic curves (Figure 7A), rate constants, and amplitudes (Table 1) obtained after unfolding for 10 min with those obtained for the equivalent single jump experiment from equilibrium unfolded β-lactamase (Figure 2A).

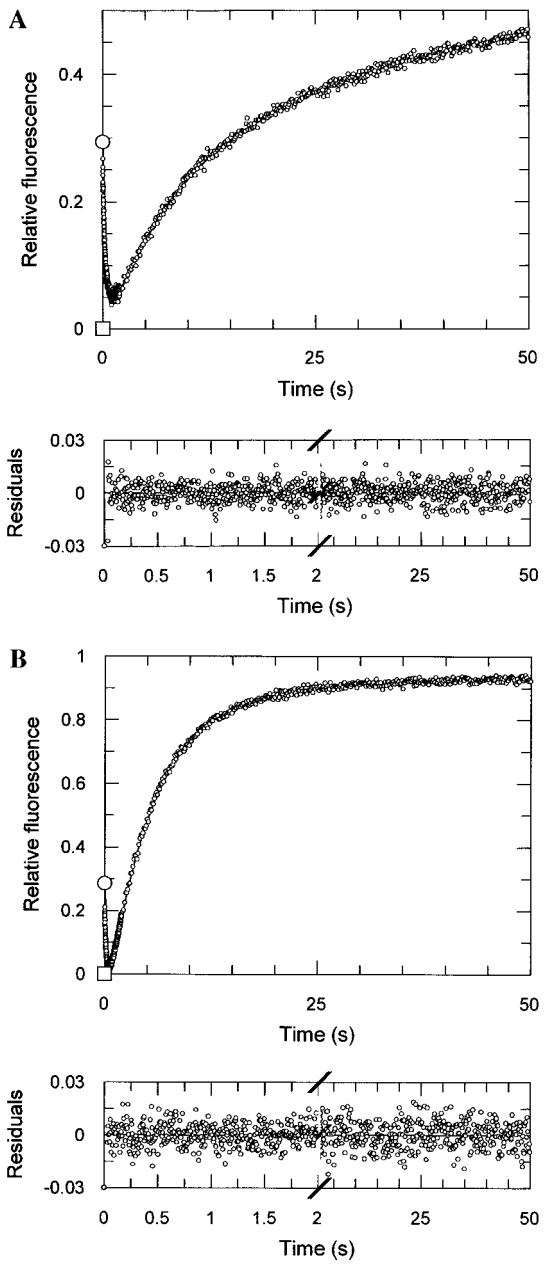

FIGURE 7: Refolding of TEM-1 β-lactamase from the unfolded chain containing Xaa−Pro bonds in their native configuration and monitored by tryptophan fluorescence. Refolding was initiated by a 6-fold dilution of the protein previously unfolded in 3 M GdmCl for 10 min (A) and 5 s (B). The signal is normalized so that the fluorescence of the unfolded state under refolding conditions is 0 (indicated by □) and that of the native enzyme is 1. The data are fitted to the sum of four exponentials, k_4 being fixed at 0.03 s^{-1} (see Materials and Methods and Table 1), and residuals are shown. (○) The value of fluorescence intensity extrapolated to zero time from the kinetic data.

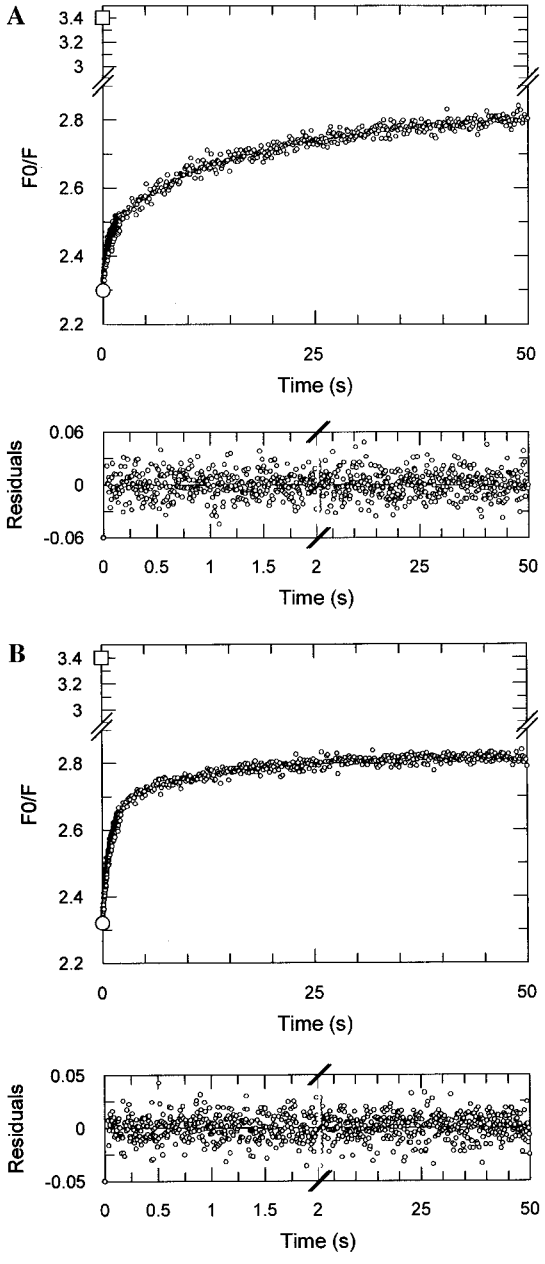

FIGURE 8: Refolding of TEM-1 β-lactamase from the unfolded chain containing Xaa−Pro bonds in their native configuration in the presence of 0.183 M acrylamide. Experimental conditions are as in Figure 7. Refolding was initiated after unfolding (A) for 10 min and (B) for 5 s. The data are fitted to the sum of four exponentials, k_4 being fixed at 0.03 s^{-1} (see Table 1), and residuals are shown. (○) F_0/F extrapolated to zero time from the kinetic data. (□) F_0/F for the unfolded protein measured as the ratio of the fluorescence values at 3 M GdmCl, with and without acrylamide.

Refolding after unfolding for 10 min, 5 min, and 5 s resulted in kinetic curves and constants for the trimodal change in intrinsic fluorescence that are similar, the shorter delay time leading to marginally faster refolding (Figure 7 and Table 1). Similar experiments, in which refolding takes place in the presence of acrylamide, showed rather similar kinetics for the change in exposure of tryptophan to solvent, this time with the longer delay time leading to slightly faster folding (Figure 8 and Table 1). Again, a marked decrease in tryptophan exposure occurs in the burst phase, followed by slower increases after about 100 ms.

DISCUSSION

TEM-1 β-lactamase comprises one all-α domain and one α/β moiety (Figure 1) with the active site situated at the junction between the two (*45*, *46*). The α/β moiety is composed of two chains coming from the N- and C-terminal ends of the α-domain which intertwine to form a β-pleated sheet. This makes for particular demands on the pathway of folding. The enzyme contains 12 prolyl residues and a single disulfide bond which connects Cys77 and Cys123 in the all-α domain. In previous reports, TEM-1 β-lactamase was shown to fold via two major parallel pathways, both being rate-limited by Xaa−Pro bond isomerization (*40*, *50*).

The slower of these two phases was ascribed to the trans to cis isomerization of the Glu166−Pro167 bond in the Ω-loop (*50*).

The use of a variety of spectroscopic probes, including fluorescence quenching, to follow the fast and slow kinetics of folding of this enzyme has provided further support for initial steps of rapid (sub millisecond) hydrophobic collapse and formation of substantial amounts of secondary structure.

Nonnative Interactions in a Burst Phase Intermediate. Like most proteins studied so far (ref *54*, p 47), TEM-1 β-lactamase acquires a substantial proportion of its native ellipticity in the far-UV during the burst phase. It remains to be seen whether, in this protein, this represents secondary structure that is nativelike with stable hydrogen bonding as in ubiquitin (*6*, *54*), nativelike with nonstable hydrogen bonding as in interleukin-1β (*12*), or at least partially nonnative as in β-lactoglobulin (*33*). What is clear is that, at the end of the burst phase, secondary structure is formed in an intermediate which exhibits increased aromatic fluorescence, decreased access of acrylamide to aromatic residues, and substantial ANS binding. The maximal binding of ANS occurs within the burst phase, significantly earlier than is generally seen in other proteins (*17*, *31*, *49*), consistent with an early hydrophobic collapse and suggesting a relatively greater stability for this intermediate. The large increase in intrinsic fluorescence marks a significant change in the environment of one or more tryptophans which the quenching experiments show to be less accessible in the burst intermediate than in the folded protein, in which they are largely exposed to the solvent.

These nonnative hydrophobic interactions, indicative of a nonhierarchical folding pathway, are similar in principle to those demonstrated in the folding of lysozyme (*10*, *20*, *34*, *35*) where their subsequent disruption accounts for the rate-limiting step in the folding (*35*). In the case of β-lactamase, the nonnative interactions are detected only because tryptophan is involved and, in addition, would probably not be seen if the tryptophans were buried in the native state. It is possible, therefore, as pointed out by Rothwarf and Scheraga (*35*), that such nonhierarchical pathways are more common than is presently recognized.

Subsequent Folding Events. The results summarized in Table 1 show that the folding of TEM-1 β-lactamase that follows the burst phase is a complex process that can be decomposed into at least five measurable phases. It is known that reactivation, which occurs in the two final phases, is rate-limited by proline isomerization (*40*, *50*). Thus, folding should occur in at least two parallel folding pathways, but it is not yet possible to assign each measured kinetic phase to a given pathway. The close similarity of the rate constants measured by complementary probes shows, however, that they represent well-defined, cooperative folding transitions.

Following the increase of the intrinsic fluorescence in the burst phase, a rapid reduction occurs in two exponential phases, before finally rising again to the emission intensity of the native protein. This results in a minimum in fluorescence intensity at approximately 800 ms under these conditions of folding. Taking into account the different conditions of temperature and folding buffer, this minimum almost certainly corresponds to that observed by Gervasoni and Plückthun (*55*). By studying the folding of the C77A and C123A mutant enzyme, these authors have assigned the quenching of fluorescence prior to the minimum to the location of W210 close to its native topology in a hydrophobic environment next to the wild-type enzyme disulfide bond.

The monotonic increase in acrylamide quenching following the burst phase must therefore be assigned to the increasing exposure to solvent of one or more tryptophan residues other than W210. An attractive model would involve the C-terminal W290 being buried in a nonnative conformation in the burst phase. The structure of β-lactamase (*45*, *46*) suggests that early intermediates take the form of a collapsed and partially folded (molten globule-like) α-domain, with its N- and C-terminal extensions probably collapsed but not yet intertwined in the native β-sheet structure of the α/β domain (it is not possible to "unfold" the α/β domain by pulling either the N- or the C-terminal residues without disrupting the whole domain at an early stage, in contrast to the α-domain). In this dynamic structure, the C-terminal tryptophan could well find a lower energy state by becoming buried in the hydrophobically collapsed α-domain. To fold and generate the native α- and β-secondary structure, this tryptophan would have to be extracted from the α-domain core and become exposed to solvent. This would be consistent with the observed slower formation of 35−40% of the native ellipticity, complete in about 60 s, prior to the final, Xaa-Pro isomerization dependent changes in tertiary structure.

The double jump experiments show that the early steps in folding are unaffected by the isomerization state of the proline residues. The conformations of the intermediates that accumulate transiently in the early stages of folding must therefore be sufficiently loosely packed for the stereochemistry of the proline residues not to lead to significant differences in their stability.

The increase in intrinsic fluorescence which characterizes the final three phases could result from formation of a Trp−Trp interaction. The equilibrium intermediate state H and the fully unfolded protein both exhibit significantly lower fluorescence quantum yields relative to the native enzyme (*40*). This could be due to the close interaction of tryptophans 229 and 290 in the native state. An analogous interaction of His18 and Trp94 in barnase has been shown to lead to a marked change in quantum yield (*56*).

ACKNOWLEDGMENT

We thank Drs. Paulette Charlier and Josette Lamotte-Brasseur for Figure 1.

REFERENCES

1. Baldwin, R. L. (1993) *Curr. Opin. Struct. Biol. 3*, 84−91.
2. Matthews, B. W. (1993) *Annu. Rev. Biochem. 62*, 139−160.
3. Evans, P. A., and Radford, S. E. (1994) *Curr. Opin. Struct. Biol. 4*, 100−106.
4. Jackson, S. E., and Fersht, A. R. (1991a) *Biochemistry 30*, 10428−10435.
5. Jackson, S. E., and Fersht, A. R. (1991b) *Biochemistry 30*, 10436−10443.
6. Briggs, M. S., and Roder, H. (1992) *Proc. Natl. Acad. Sci. U.S.A. 89*, 2017−2021.
7. Kragelund, B. B., Robinson, C. V., Knudsen, J., Dobson, C. M., and Poulsen, F. M. (1995) *Biochemistry 34*, 7117−7224.
8. Schindler, T., Herrler, M., Marahiel, M. A., and Schmid, F. X. (1995) *Nat. Struct. Biol. 2*, 663−673.

9. Bycroft, M., Matouschek, A., Kellis, J. T., Serrano, L., and Fersht, A. R. (1990) *Nature 346*, 488−490.
10. Radford, S. E., Dobson, C. M., and Evans, P. A. (1992) *Nature 358*, 302−307.
11. Jennings, P. A., and Wright, P. E. (1993) *Science 262*, 892−895.
12. Varley, P., Gronenborn, A. M., Christensen, H., Wingfield, P. T., Pain, R. H., and Clore, M. (1993) *Science 260*, 1110−1113.
13. Udgaonkar, J. E., and Baldwin, R. L. (1988) *Nature 335*, 694−699.
14. Roder, H., Elöve, G. A., and Englander, S. W. (1988) *Nature 335*, 700−704.
15. Miranker, A., Robinson, C. V., Radford, S. E., Aplin, R. T., and Dobson, C. M. (1993) *Science 262*, 896−899.
16. Ikeguchi, M., Kuwajima, K., Mitani, M., and Sugai, S. (1986) *Biochemistry 25*, 6965−6972.
17. Ptitsyn, O. B., Pain, R. H., Semisotnov, G. V., Zerovnik, E., and Razgulyaev, O. I. (1990) *FEBS Lett. 262*, 20−24.
18. Elöve, G. A., Chaffotte, A. F., Roder, H., and Goldberg, M. E. (1992) *Biochemistry 31*, 6876−6883.
19. Chaffotte, A. F., Guillou, Y., and Goldberg, M. E. (1992) *Biochemistry 31*, 9694−9702.
20. Itzhaki, L. S., Evans, P. A., Dobson, C. M., and Radford, S. E. (1994) *Biochemistry 33*, 5212−5220.
21. Cummings, A. L., and Eyring, E. M. (1975) *Biopolymers 14*, 2107−2114.
22. Zana, R. (1975) *Biopolymers 14*, 2425−2428.
23. Karplus, M., and Weaver, D. L. (1976) *Nature 260*, 404−406.
24. Kim, P. S., and Baldwin, R. L. (1990) *Annu. Rev. Biochem. 59*, 631−660.
25. Karplus, M., and Weaver, D. L. (1994) *Protein Sci. 3*, 650−668.
26. Chan, H. S., and Dill, K. A. (1990) *Proc. Natl. Acad. Sci. U.S.A. 87*, 6388−6392.
27. Covell, D. G., and Jernigan, R. L. (1990) *Biochemistry 29*, 3287−3294.
28. Neri, D., Billeter, M., Wider, G., and Wüthrich, K. (1992) *Science 257*, 1559−1563.
29. Saab-Rincon, G., Froebe, C. L., and Matthews, C. R. (1993) *Biochemistry 32*, 13981−13990.
30. Uversky, V. N., and Ptitsyn, O. B. (1994) *Biochemistry 33*, 2782−2791.
31. Semisotnov, G. V., Rodionova, N. A., Razgulyaev, O. I., Uversky, V. N., Gripas, A. F., and Gilmanshin, R. I. (1991) *Biopolymers 31*, 119−128.
32. Eaton, W. A., Thompson, P. A., Chan, C.-K., Hagen, S. J., and Hofrichter, J. (1996) *Structure 4*, 1133−1139.
33. Hamada, D., Segawa, S., and Goto, Y. (1996) *Nat. Struct. Biol. 3*, 868−873.
34. Denton, M. E., Rothwarf, D. M., and Scheraga, H. A. (1994) *Biochemistry 33*, 11225−11236.
35. Rothwarf, D. M., and Scheraga, H. A. (1996) *Biochemistry 35*, 13797−13807.
36. Brent, R., and Ptashne, M. (1981) *Proc. Natl. Acad. Sci. U.S.A. 78*, 4204−4208.
37. Dubus, A., Wilkin, J.-M., Raquet, X., Normark, S., and Frère, J.-M. (1994) *Biochem. J. 301*, 485−494.
38. Nozaki, Y. (1972) *Methods Enzymol. 26*, 43−50.
39. Tonomura, B., Nakatani, H., Ohnishi, M., Yamaguchi-Ito, J., and Hiromi, K. (1978) *Anal. Biochem. 84*, 370−383.
40. Vanhove, M., Raquet, X., and Frère, J.-M. (1995) *Proteins: Struct., Funct., Genet. 22*, 110−118.
41. Lakowicz, J. R. (1986) *Principles of Fluorescence Spectroscopy*, Plenum Press, New York.
42. Eftink, M. R. (1991) *Methods Biochem. Anal. 35*, 127−207.
43. Lehrer, S. S. (1971) *Biochemistry 10*, 3254−3263.
44. Garvey, E. P., Swank, K., and Matthews, C. R. (1989) *Proteins: Struct., Funct., Genet. 6*, 259−266.
45. Jelsch, C., Mourey, L., Masson, J.-M., and Samama, J.-P. (1993) *Proteins: Struct., Funct., Genet. 16*, 364−383.
46. Strynadka, N. C. J., Adachi, H., Jensen, S. E., Johns, K., Sielecki, A., Betzel, C., Sutoh, K., and James, M. N. J. (1992) *Nature 359*, 700−705.
47. Eftink, M. R., and Ghiron, C. A. (1981) *Anal. Biochem. 114*, 672−680.
48. Birks, J. B. (1970) *Photophysics of Aromatic Molecules*, pp 433−447, Wiley-Interscience, New York.
49. Jones, B. E., Jennings, P. A., Pierre, R. A., and Matthews, C. R. (1994) *Biochemistry 33*, 15250−15258.
50. Vanhove, M., Raquet, X., Palzkill, T., Pain, R. H., and Frère, J.-M. (1996) *Proteins: Struct., Funct., Genet. 25*, 104−111.
51. Brandts, J. F., Halvorson, H. R., and Brennan, M. (1975) *Biochemistry 14*, 4953−4960.
52. Schmid, F. X. (1993) *Annu. Rev. Biophys. Biomol. Struct. 22*, 123−143.
53. Mitchinson, C., and Pain, R. H. (1985) *J. Mol. Biol. 184*, 331−342.
54. Roder, H., and Elöve, G. A. (1994) in *Mechanisms of Protein Folding* (Pain, R. H., Ed.) pp 26−54, Oxford University Press, Oxford, U.K.
55. Gervasoni, P., and Plückthun, A. (1997) *FEBS Lett. 401*, 138−142.
56. Loewenthal, R., Sancho, J., and Fersht, A. R. (1991) *Biochemistry 30*, 6775−6779.

BI972143C